Assessment of Influential Parameters in Topology Optimization of Thermo-Mechanically Loaded Concrete Structures

Ticho Ooms, Ruben Van Coile, and Wouter De Corte(✉)

Department of Structural Engineering and Building Materials, Ghent University, Ghent, Belgium
Wouter.DeCorte@UGent.be

Abstract. Topology optimization (TO) is a powerful technique for the optimization of structural components, without a priori knowledge of the material distribution in a given design domain and for a predetermined set of objectives and constraints. In case of building structures many TO procedures have been developed for structural efficiency in various load scenarios, however few studies exist where thermal loading due to fire is considered. Therefore, in this study a compliance-based TO procedure is presented in which the effect of fire loading is taken into account by imposing thermo-mechanical loading, governed by thermal expansion, on a structure. The proposed TO procedure is employed to compare the results of different assumptions for the thermo-mechanical model. The results show large discrepancies between the assumption of steady-state versus transient heat transfer. Moreover, an increasing time period in case of transient heat transfer affects the results significantly due to the increased contribution of thermal loading. Furthermore, the ratio of thermal to mechanical loading strongly influences the resulting topologies and a realistic load scenario is thermally dominant with respect to the compliance objective. In summary, this study shows the importance of the assumption of transient heat transfer in the optimization as well as careful assessment of the thermo-mechanical loading.

Keywords: Fire safety · Structural Efficiency · Thermo-mechanical loading · Topology Optimization · Transient heat conduction

1 Introduction

Structures are not only affected by mechanical loads but also by a range of other influences such as thermal loading caused by temperature changes or fire exposure. In order to optimize structural components for fire safety, a performance-based approach that takes into account the influence of elevated temperatures is beneficial. However, fire loading is a transient thermal phenomenon with a complex stress field due to thermal expansion, making it difficult to carry out the sensitivity analysis in a gradient-based topology optimization procedure. Topology optimization for thermo-mechanical loading has been discussed in literature [1, 2], but few research papers have been published

A. Ilki et al. (Eds.): *fib* Symposium 2023, LNCE 350, pp. 119–127, 2023.
https://doi.org/10.1007/978-3-031-32511-3_14

on topology optimization with fire loading [3]. This paper discusses a topology optimization procedure that considers the influence of elevated temperatures through both steady-state and transient heat conduction for structures exposed to fire and its influential parameters. A case study of a simply supported beam subjected to thermo-mechanical loads is presented and discussed. The effect of transient thermal analysis is investigated in comparison to steady-state heat transfer, including the influence for the time period and time increment. Furthermore, it is shown that the thermo-mechanical load ratio significantly influences the resulting topologies.

2 Topology Optimization with Thermo-Mechanical Loads

2.1 Optimization Problem

The optimization problem in this study involves the minimization of structural compliance c (maximizing stiffness) while being subjected to a volume constraint V with a prescribed volume fraction φ of the initial volume V_0, as expressed in Eq. (1) for the steady-state heat conduction (SHC) case. The design variables are the relative densities x_e for each element e.

The thermo-mechanical response is governed by sequentially coupled thermal and mechanical analyses $\boldsymbol{K}_{th}\boldsymbol{T} = \boldsymbol{Q}$ and $\boldsymbol{K}\boldsymbol{U} = \boldsymbol{F}_m + \boldsymbol{F}_{th}$ respectively, where $\boldsymbol{K}_{th}$ is the thermal stiffness matrix, $\boldsymbol{T}$ is the temperature field, $\boldsymbol{Q}$ is the heat load vector, $\boldsymbol{K}$ is the stiffness matrix, $\boldsymbol{U}$ is the displacement field and $\boldsymbol{F} = \boldsymbol{F}_m + \boldsymbol{F}_{th}$ is the load vector comprised of the mechanical and thermal contributions.

$$\mathbb{TO}_1 \begin{cases} \text{Find} & \boldsymbol{x} = \left(x_1, x_2, \ldots x_{N_e}\right) \\ \min\limits_{x} & c = \boldsymbol{F}^T\boldsymbol{U} \\ \text{s.t.} & V = V(\boldsymbol{x}) - \varphi V_0 \leq 0 \\ & \boldsymbol{K}_{th}\boldsymbol{T} = \boldsymbol{Q} \\ & \boldsymbol{K}\boldsymbol{U} = \boldsymbol{F} = \boldsymbol{F}_m + \boldsymbol{F}_{th} \\ & 0 \leq x_e \leq 1 \qquad \forall x_e \in \boldsymbol{x} \end{cases} \tag{1}$$

Similarly, the topology optimization formulation for the transient thermal load case is expressed in Eq. (2). Here, the compliance is a total measure taking into account the compliance in each time step $t \in [0, t_N]$ of the entire time period t_f for the thermo-mechanical analysis. In the transient thermal state equation $\boldsymbol{C}\dot{\boldsymbol{T}} + \boldsymbol{K}_{th}\boldsymbol{T} = \boldsymbol{Q}$, $\boldsymbol{C}$ is the heat capacity matrix and $\dot{\boldsymbol{T}}$ is the time-derivative of the temperature field.

$$\mathbb{TO}_2 \begin{cases} \text{Find} & \boldsymbol{x} = \left(x_1, x_2, \ldots x_{N_e}\right) \\ \min\limits_{x} & c = \sum_{t=0}^{t_N} \boldsymbol{F}^{(t)^T}\boldsymbol{U}^{(t)} \quad t_N = t_f/\Delta t \\ \text{s.t.} & V = V(\boldsymbol{x}) - \varphi V_0 \leq 0 \\ & \boldsymbol{C}\dot{\boldsymbol{T}} + \boldsymbol{K}_{th}\boldsymbol{T} = \boldsymbol{Q} \\ & \boldsymbol{K}\boldsymbol{U} = \boldsymbol{F} = \boldsymbol{F}_m + \boldsymbol{F}_{th} \\ & 0 \leq x_e \leq 1 \qquad \forall x_e \in \boldsymbol{x} \end{cases} \tag{2}$$

The governing equation for the transient heat conduction (THC) is discretized with respect to time with an implicit backward Euler scheme into t_N time increments of size Δt.

2.2 Material Interpolation

A two-phase material is considered with a solid ($x_e = 1$) and void ($x_e = 0$) phase. In order to employ a gradient-based optimizer, the material properties are expressed as a function of the relative density x_e. In this study, the SIMP approach [4] is used for each material property M with penalization factor $p_M = 3$, as expressed in Eq. (3). Herein, M_1 and M_0 are the values for the solid and void material phases respectively.

$$M(x_e) = M_0 + x_e^{p_M}(M_1 - M_0) \tag{3}$$

For the THC case, the specific heat capacity c_p and the volumetric density ρ are linearly interpolated without penalization for intermediate densities.

In addition to the standard material properties, the thermal stress coefficient (TSC) $\beta = E\alpha$ is separately penalized in the thermo-mechanical load vector $\boldsymbol{F}_{th}$ based on Gao et al. [5].

2.3 Sensitivity Analysis

The presented topology optimization procedure employs the method of moving asymptotes (MMA) [6] as the gradient-based optimizer to update the design variables. Herein, sensitivity information for the objective function and the volume constraint is required. For an efficient implementation of the sensitivity analysis, the adjoint method is used to obtain an analytical expression for the compliance sensitivities [4]. For the sensitivity of the volume constraint the reader is referred to [7]. For further details on the derivation of the compliance sensitivity, see [8].

Steady-State Heat Conduction (SHC). The sensitivity of the compliance objective in the case of SHC consists of three terms, as shown in Eq. (4). The first term is the structural compliance as expected for a mechanical load only. The second term takes into account the influence of the design-dependent thermal load and the third term contains the sensitivity of the thermal conductivity.

$$\frac{dc}{d\boldsymbol{x}} = -\boldsymbol{U}^T \frac{\partial \boldsymbol{K}}{\partial \boldsymbol{x}} \boldsymbol{U} + 2\boldsymbol{U}^T \frac{\partial \boldsymbol{F}}{\partial \boldsymbol{x}} + \boldsymbol{\mu}^T \frac{\partial \boldsymbol{K}_{th}}{\partial \boldsymbol{x}} \boldsymbol{T} \tag{4}$$

In the third term of $dc/d\boldsymbol{x}$ in Eq. (4), the adjoint variable $\boldsymbol{\mu}$ is calculated as the solution to the adjoint system in Eq. (5). Apart from the thermal and mechanical equilibrium, the adjoint problem is the third linear system of equations that is solved each iteration of the optimization process.

$$\boldsymbol{\mu} = \boldsymbol{K}_{th}^{-1} \left(-2\boldsymbol{U}^T \frac{\partial \boldsymbol{F}}{\partial \boldsymbol{T}} \right) \tag{5}$$

Transient Heat Conduction (THC). The sensitivity of the compliance objective in the case of THC has a similarities with Eq. (4) with subtle differences with respect to the time-dependency. Moreover, the sensitivities take into account the complete load history throughout the entire time period t_f. The first sum in the right hand side of Eq. (6) contains the sensitivity of the stiffness matrix and the design-dependent thermal loads.

The second sum is more elaborate and deals with the influence of the design variables on the heat capacity and conductivity, and it is dependent on the temperature fields at two consecutive time steps. Both terms consists of the accumulated contributions for each time step.

$$\begin{aligned}\frac{dc}{d\boldsymbol{x}} = &\sum_{t=0}^{t_N}\left(-\boldsymbol{U}^{(t)}\frac{\partial \boldsymbol{K}}{\partial \boldsymbol{x}}\boldsymbol{U}^{(t)} + \frac{\partial \boldsymbol{F}^{(t)^T}}{\partial \boldsymbol{x}}\boldsymbol{U}^{(t)}\right) \\ &+\sum_{t=1}^{t_N}\boldsymbol{\mu}^{(t)^T}\left(\left(\frac{1}{\Delta t}\frac{\partial \boldsymbol{C}}{\partial \boldsymbol{x}} + \frac{\partial \boldsymbol{K}_{th}}{\partial \boldsymbol{x}}\right)\boldsymbol{T}^{(t)} - \frac{1}{\Delta t}\frac{\partial \boldsymbol{C}}{\partial \boldsymbol{x}}\boldsymbol{T}^{(t-1)}\right)\end{aligned} \tag{6}$$

The adjoint variables $\boldsymbol{\mu}^{(t)}$ in Eq. (7) are derived in a similar fashion as Eq. (4), however, due to the time-dependency, backward calculation from time step t_N to 1 is required.

$$\begin{aligned}\boldsymbol{\mu}^{(t)} &= \left(\tfrac{1}{\Delta t}\boldsymbol{C} + \boldsymbol{K}_{th}\right)^{-1}\left(-2\boldsymbol{U}^{(t)}\frac{\partial \boldsymbol{F}^{(t)^T}}{\partial \boldsymbol{T}^{(t)}}\right) && t = t_N \\ \boldsymbol{\mu}^{(t)} &= \left(\tfrac{1}{\Delta t}\boldsymbol{C} + \boldsymbol{K}_{th}\right)^{-1}\left(\boldsymbol{\mu}^{(t+1)^T}\tfrac{1}{\Delta t}\boldsymbol{C} - 2\boldsymbol{U}^{(t)}\frac{\partial \boldsymbol{F}^{(t)^T}}{\partial \boldsymbol{T}^{(t)}}\right) && t = 1, \ldots, t_N - 1\end{aligned} \tag{7}$$

The adjoint system in Eq. (7) needs to be solved for every time step in each iteration. Therefore, the time increment directly influences the computation time of the sensitivities as the number of linear systems to be solved per iteration equals $3 \times t_N$.

3 Results and Discussion

3.1 Problem Description

The implementation of both SHC and THC approaches is demonstrated on the example of a simply supported beam in three point bending, extended with thermal boundary conditions. By default, the point load is $10kN$ and the thermal Dirichlet conditions are $T_a = 20\,°\text{C}$ and $T_f = 800\,°\text{C}$. Furthermore, a volume constraint of 40% is imposed. Due to symmetry only half of the beam is modelled for computational efficiency. More details on the dimensions are provided in Fig. 1.

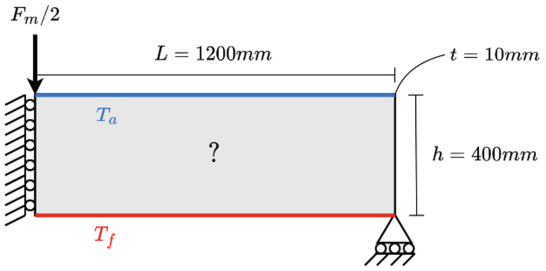

Fig. 1. Simply supported beam subjected to a point load and thermal boundary conditions

The material properties are listed in Table 1. In the solid phase the material resembles concrete and in the void phase a fictitious, very weak insulation material is considered.

Table 1. Two-phase material properties for concrete – insulation

$E_1 - E_0$ $[MPa]$	ν $[-]$	α $[1/K]$	$\kappa_1 - \kappa_0$ $[W/mK]$	$c_{p,1} - c_{p,0}$ $[J/kgK]$	$\rho_1 - \rho_0$ $[kg/m^3]$
30e3 − 30e−6	0.3	12e−6	1 − 0.03	900 − 800	2400 − 1

A Heaviside projection filter with a filter radius of 3 is used to avoid checkerboarding and mesh dependency issues [4, 7].

3.2 Steady-State Versus Transient Heat Conduction

Influence of the Time Period. In this section, the time period for the thermal analysis is varied from 1 to 24 h, including the steady-state analysis. The time period for the thermal analysis directly influences the temperature field and therefore also the thermo-mechanical loading. The optimized results are shown in Fig. 2.

All results in Fig. 2 are characterized by a insulating region at the bottom of the design domain. This zone prevents thermal energy from propagating into the solid structure and further limits thermal deformation of the structure. Naturally, the zone forms as the thermal boundary conditions are not design-dependent and remain stationary at the initial location. The extent of the insulating region is proportional to the magnitude of the thermal loading and grows for an increasing time period. As the time period further increases to infinity the results for the steady-state (Fig. 2d) and transient implementations naturally coincide.

Influence of the Time Increment. The optimization procedure considering THC is carried for a time period of $1h$ with default thermo-mechanical loading, i.e. $T_f = 800\,°C$ and $F_m = 10\,kN$, and time increments Δt of 3600 s, 900 s, 36 s and 10 s.

The results for various time steps show slight differences due to local optima and as a consequence of a slightly different temperature field (see Fig. 3). Nevertheless, the use of a large time increment (e.g. $\Delta t = t_f/4$) is acceptable for a preliminary design, partly

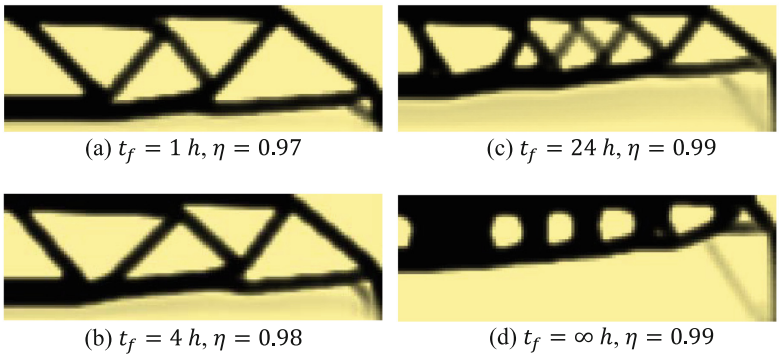

(a) $t_f = 1\ h, \eta = 0.97$ (c) $t_f = 24\ h, \eta = 0.99$

(b) $t_f = 4\ h, \eta = 0.98$ (d) $t_f = \infty\ h, \eta = 0.99$

Fig. 2. Optimized results for various time periods

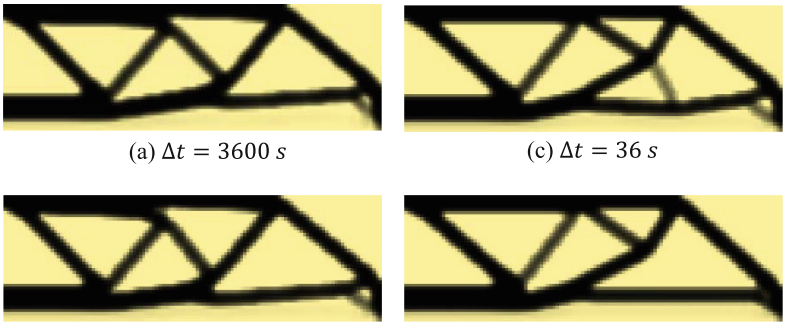

(a) $\Delta t = 3600\ s$ (c) $\Delta t = 36\ s$

(b) $\Delta t = 900\ s$ (d) $\Delta t = 10\ s$

Fig. 3. Optimized results for various time increments

due to the implicit discretization scheme, and preferred for computational efficiency. For a more accurate assessment of the temperature field and the resulting topology, a smaller time increment can offer a better solution at an increased computational cost.

3.3 Influence of Thermo-Mechanical Load Ratio

The thermo-mechanical load ratio (TMLR) for the SHC case η_{SHC} can be quantitatively expressed as the ratio of the thermal contribution c_{th} to the total structural compliance c_{tot} for a solid design ($\boldsymbol{x} = 1$) in Eq. (8).

$$\eta_{SHC} = \frac{c_{th}}{c_{tot}} \tag{8}$$

Herein, $c_{th} = \boldsymbol{F}_{th}^{T}\boldsymbol{U}$ and $c_{tot} = \boldsymbol{F}^{T}\boldsymbol{U}$ with $\boldsymbol{U}$ the global displacement vector resulting from the combined thermo-mechanical action for the SHC case. An equivalent expression is used for the THC case.

Variable Thermal Gradient. The TMLR is first changed by varying the thermal gradient with T_f ranging from 20 °C to 800 °C with a constant mechanical load $F_m = 10kN$.

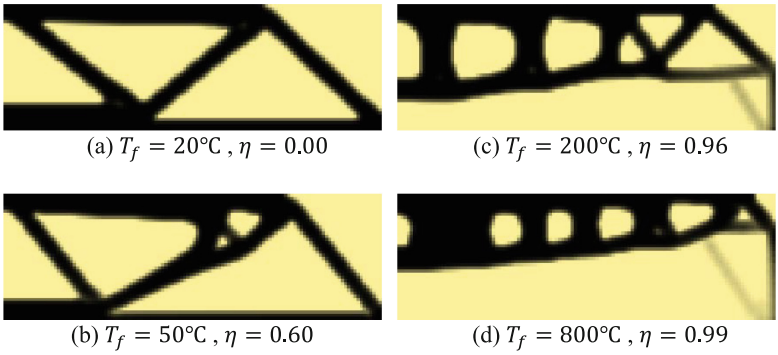

(a) $T_f = 20$°C , $\eta = 0.00$ (c) $T_f = 200$°C , $\eta = 0.96$

(b) $T_f = 50$°C , $\eta = 0.60$ (d) $T_f = 800$°C , $\eta = 0.99$

Fig. 4. Optimized results for various thermal gradients (SHC)

In Fig. 4, the results show how the thermal loading significantly changes the resulting topology. As the TMLR switches from mechanically dominant ($\eta < 0.5$) to thermally dominant ($\eta > 0.5$), the insulating region enlarges and the truss structure is transformed into a cellular beam on top of the insulation.

Similar results are observed in the case of THC, as illustrated in Fig. 5, albeit with a less extreme transformation for a time period of 1 h. The steady-state assumption is more severe than the transient case for construction materials such as concrete, having a small thermal diffusivity. Therefore, it is advised to implement THC instead of SHC for the design optimization of concrete components taking into account thermal effects.

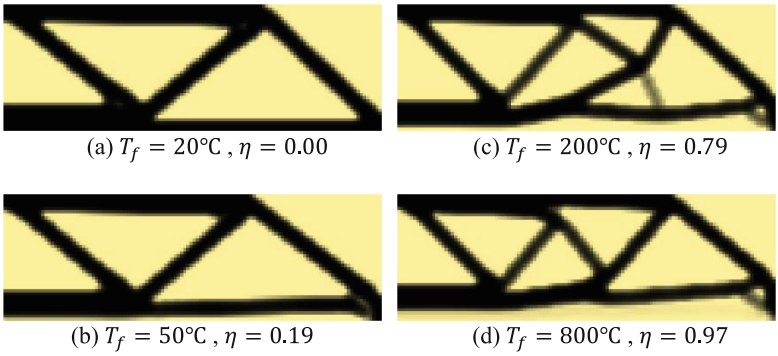

(a) $T_f = 20$°C , $\eta = 0.00$ (c) $T_f = 200$°C , $\eta = 0.79$

(b) $T_f = 50$°C , $\eta = 0.19$ (d) $T_f = 800$°C , $\eta = 0.97$

Fig. 5. Optimized results for various thermal gradients (THC)

Variable Mechanical Load. The second approach for changing the TMLR is by varying the mechanical load (with a constant thermal gradient). Here, the mechanical load ranges from 0 kN to 1000 kN.

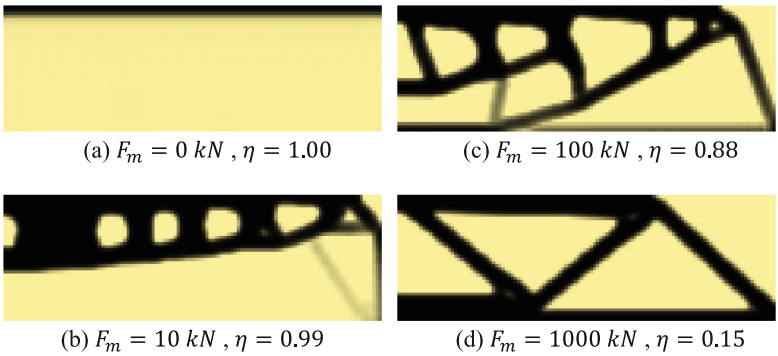

(a) $F_m = 0\ kN$, $\eta = 1.00$ (c) $F_m = 100\ kN$, $\eta = 0.88$

(b) $F_m = 10\ kN$, $\eta = 0.99$ (d) $F_m = 1000\ kN$, $\eta = 0.15$

Fig. 6. Optimized results for various mechanical loads (SHC)

The results in Fig. 6 (for SHC) and Fig. 7 (for THC) show a similar trend as the case with a variable thermal gradient. However, the results for the absence of the mechanical load (see Fig. 6a and Fig. 7a) are unstable and the volume constraint appears to be inactive. The optimized topology is entirely dependent on the TMLR and therefore it is important to accurately assess the thermo-mechanical loading on the structure, including multiple load cases.

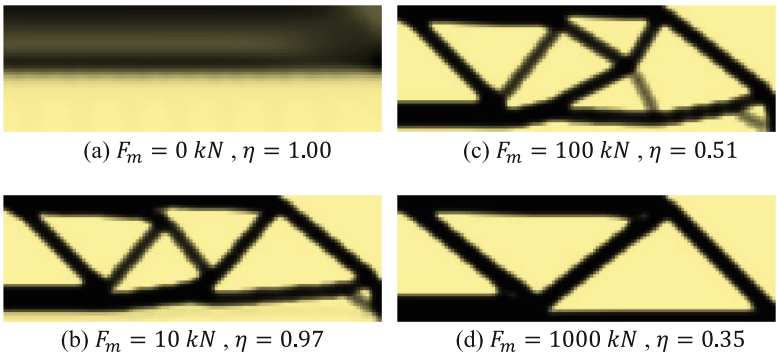

(a) $F_m = 0\ kN$, $\eta = 1.00$ (c) $F_m = 100\ kN$, $\eta = 0.51$

(b) $F_m = 10\ kN$, $\eta = 0.97$ (d) $F_m = 1000\ kN$, $\eta = 0.35$

Fig. 7. Optimized results for various mechanical loads (THC)

In case the out-of-plane thickness is changed in the mechanical analysis, the TMLR is also influenced. However, as this is inversely proportional to changing the mechanical load, a variable thickness is disregarded here. For example, the mechanical response of

a structure with a thickness of 1 mm and a point load of 10 kN will be equal to that of the same structure with a thickness of 10 mm and a point load of 100 kN.

Variable Time Period. As demonstrated in Sect. 3.1 and indicated by the TMLR in Fig. 4, the time period influences the thermo-mechanical loading. As the thermal gradient is sustained for a longer period of time, the propagation of thermal energy in the structure is amplified.

4 Conclusions

In this study, a topology optimization procedure for structural components in concrete subjected to thermo-mechanical loads considering steady-state and transient heat conduction is presented. The results show that the difference between the assumption of the steady-state and transient heat transfer is significant, as the steady-state assumption is more severe and less realistic. Both the time period and the time step influence the results as the temperature field is directly affected by these parameters. Furthermore, careful assessment of the thermo-mechanical load ratio (TMLR) is important as the optimized topology is entirely determined by the TMLR. Other parameters that influence the results are the time period for the transient thermal analysis and the out-of-plane thickness in the mechanical analysis.

The authors acknowledge the simplified assumptions for the behavior of concrete. Therefore, future work is dedicated to extending the presented optimization strategy with more realistic thermal and mechanical material properties of (reinforced) concrete, e.g., as described in Eurocode 2. Further research will be focused on the implementation of temperature-dependent properties and elastoplastic behavior of concrete, as well as the feasibility of including reinforcement in the optimization procedure.

References

1. Deaton JD, Grandhi R (2014) A survey of structural and multidisciplinary continuum topology optimization: Post 2000. Struct Multidiscip Optim 49(1):1–38. https://doi.org/10.1007/s00158-013-0956-z
2. Leader MK (2021) Stress-based topology optimization for steady-state and transient thermoelastic design Ph.D. thesis
3. Madsen S, Lange NP, Giuliani L, Jomaas G, Lazarov BS, Sigmund O (2016) Topology optimization for simplified structural fire safety. Eng Struct 124:333–343
4. Bendsøe M, Sigmund O (2003) Topology optimization: theory, methods and applications. Springer, Heidelberg. https://doi.org/10.1007/978-3-662-05086-6
5. Gao T, Zhang W (2010) Topology optimization involving thermo-elastic stress loads. Struct Multidiscip Optim 42(5):725–738. https://doi.org/10.1007/s00158-010-0527-5
6. Svanberg K (1987) The method of moving asymptotes - a new method for structural optimization. Int J NumerMethods Eng 24(2):359–373
7. Andreassen E, Clausen A, Schevenels M, Lazarov BS, Sigmund O (2011) Efficient topology optimization in MATLAB using 88 lines of code. Struct Multidiscip Optim 43(1):1–16. https://doi.org/10.1007/s00158-010-0594-7
8. Ooms T, Vantyghem G, Thienpont T, Van Coile R, De Corte W (2023) Compliance-based topology optimization of structural components subjected to thermo-mechanical loading. Struct Multidiscip Optim (Under review)